

# Mapping Structural Brain Alterations in Obsessive-Compulsive Disorder

Jesús Pujol, MD; Carles Soriano-Mas, PhD; Pino Alonso, MD; Narcís Cardoner, MD; José M. Menchón, MD; Joan Deus, PhD; Julio Vallejo, MD

**Background:** Recent technical developments have made it feasible to comprehensively assess brain anatomy in psychiatric populations.

**Objective:** To describe the structural brain alterations detected in the magnetic resonance images of a large series of patients with obsessive-compulsive disorder (OCD) using imaging procedures that allow the evaluation of volume changes throughout the brain.

**Design:** Case-control study.

**Setting:** Referral OCD unit in a tertiary hospital.

**Participants:** A consecutive sample of 72 outpatients with OCD and 72 age- and sex-matched control subjects.

**Interventions:** Three-dimensional sequences were obtained in all participants. A statistical parametric mapping approach was used to delineate possible anatomical alterations in the entire brain. To preserve volumetric information, voxel values were modulated by the Jacobian determinants (volume change measurement) derived from spatial normalization.

**Main Outcome Measures:** Voxelwise brain volumes.

**Results:** The brains of patients with OCD showed reduced gray matter volume in the medial frontal gyrus, the medial orbitofrontal cortex, and the left insulo-opercular region. A relative increase in gray matter volume was observed bilaterally in the ventral part of the putamen and in the anterior cerebellum. All these brain alterations were abnormally correlated in patients with OCD, and age statistically significantly contributed to the relative enlargement observed in the striatal areas. Disease severity, the nature of symptoms, and comorbidities were not related to the changes described. Nevertheless, patients with prominent aggressive obsessions and checking compulsions showed reduced amygdala volume in the right hemisphere.

**Conclusions:** The pattern of anatomical features depicted by this voxelwise approach is consistent with data from functional studies. The reported anatomical maps identified the specific parts of the frontostriatal system that were altered in patients with OCD and detected changes in anatomically connected distant regions. These data further define the structural brain alterations in OCD and may contribute to constraining the prevailing biological models of this psychiatric process.

*Arch Gen Psychiatry. 2004;61:720-730*

From the Magnetic Resonance Center of Pedralbes (Drs Pujol and Soriano-Mas), the Department of Psychiatry, Hospital of Bellvitge, University of Barcelona (Drs Alonso, Cardoner, Menchón, and Vallejo), and the Department of Geriatrics, Sant Jaume Hospital of Mataró (Dr Deus), Barcelona, Spain.

**R**ESULTS FROM A VARIETY OF research sources have made it possible to consider the pathogenesis of obsessive-compulsive disorder (OCD) in terms of brain anatomy.<sup>1,2</sup> Neurological patients showing obsessions and compulsions generally have diseases involving the basal ganglia or the inferior frontal cortex.<sup>1-4</sup> Neuropsychological alterations in patients with OCD include deficits in the executive functions of the frontal lobes.<sup>5</sup> Neurosurgical procedures aimed at treating OCD symptoms directly or indirectly disconnect frontosubcortical loops.<sup>6</sup> Functional brain imaging reveals orbitofrontal and basal ganglia hypermetabolism in patients with OCD at rest and during symp-

tom provocation that normalizes with response to treatment.<sup>7-9</sup>

Available data, therefore, are consistent in identifying functional alterations involving frontosubcortical circuits. It is not clear, however, to what extent the altered systems show detectable changes in their anatomy. Structural neuroimaging has indeed provided some evidence of anatomical alterations in OCD, but the reported findings have been notably heterogeneous, probably as a consequence of different patient selection and the diversity of methods adopted to delineate regions of interest. Although volume reduction<sup>10-12</sup> and enlargement<sup>13-15</sup> were observed for different components of the basal ganglia and thalamus, other researchers<sup>16-19</sup> re-

ported no differences between patients and control subjects. Reduced orbitofrontal and amygdala volumes were also detected,<sup>20</sup> and alterations in distant structures, such as the cerebellum, were identified using 3-dimensional magnetic resonance imaging (MRI).<sup>21,22</sup>

The diversity of the described neuroanatomical findings suggests that imaging procedures that allow analysis of the entire cerebral parenchyma could further contribute to delimiting the distribution of prevailing structural alterations in the OCD brain, particularly if a large number of patients are assessed. Recent technical developments have made it feasible to measure direct size variations of anatomical elements on a voxel-by-voxel basis. In this study, we use a voxelwise approach to identify possible structural brain alterations in the MRIs of 72 patients with OCD. We report statistical parametric maps (SPMs) showing substantial brain tissue volume differences between patients with OCD and a comparable group of 72 controls and describe the correlations of anatomical changes with relevant clinical variables.

## METHODS

### PARTICIPANTS

Outpatients were consecutively recruited according to DSM-IV criteria for OCD and the absence of relevant medical, neurological, and other major psychiatric diseases. Specifically, no patient in this study met the criteria for Tourette syndrome or showed psychoactive substance abuse. Comorbidity with anxiety and depression symptoms was not considered an exclusion criterion provided that OCD was the primary clinical process. Diagnosis was independently assigned by 2 psychiatrists (P.A. and J.M.M.) with extensive clinical experience in OCD who separately interviewed patients using the *Structured Clinical Interview for DSM-IV Axis I Disorders—Clinician Version*.<sup>23</sup> Patients were eligible for the study when both research examiners agreed on all criteria.

Seventy-two patients composed the study group (32 women and 40 men; mean  $\pm$  SD age, 29.8  $\pm$  10.5 years; range, 18–60 years). All but 11 patients were right-handed according to the Edinburgh Inventory.<sup>24</sup> The mean  $\pm$  SD level of education attained was 13.2  $\pm$  3.6 years. **Table 1** reports the clinical characteristics of the patient sample. The Yale-Brown Obsessive-Compulsive Scale<sup>26</sup> and a clinician-rated Yale-Brown Obsessive-Compulsive Scale symptom checklist<sup>26</sup> were used to assess severity and to characterize the clinical expression of the OCD. As in other studies,<sup>25,27–30</sup> symptom severity was recorded for each checklist element. Each participant was assigned a score of 0 (absent), 1 (mild), or 2 (prominent) for each of the 5 clinical dimensions defined by Mataix-Cols et al<sup>25</sup> (Table 1). The score provided for each given dimension reflected the highest score for any of the checklist elements composing that dimension. Comorbid processes were assessed in the clinical interviews using DSM-IV criteria. Hamilton scales<sup>31,32</sup> were used to rate depression and anxiety at inclusion. Ten patients had received experimental treatment with transcranial magnetic stimulation on the frontal lobe 12 months before inclusion in this study.<sup>33</sup>

Seventy-two comparative control subjects from the same sociodemographic environment were matched to the patients by age, sex, and handedness. A detailed medical history was recorded and a psychiatric interview was administered before inclusion to exclude psychiatric disorders, adopting the guidelines established by Shtasel et al.<sup>34</sup> The selected volunteers, of whom 11 were left-handed, had a mean  $\pm$  SD age of 30.1  $\pm$  10.2 years (range, 18–57 years) and an identical sex distribution as the pa-

tient group (32 women and 40 men). The mean level of education in the control group was 14.0  $\pm$  3.1 years ( $t_{1,42} = -1.5$ ;  $P = .14$ ).

All patients and controls gave written informed consent after receiving a complete description of the study, which was approved by the institutional review board (Hospital of Bellvitge).

### MRI ACQUISITION AND PROCESSING

All imaging studies were acquired using a 1.5-T magnet (Signa; GE Medical Systems, Milwaukee, Wis). A 60-slice, 3-dimensional, spoiled gradient-recalled acquisition sequence was obtained in the sagittal plane. Acquisition parameters were as follows: repetition time, 40 milliseconds; echo time, 4 milliseconds; pulse angle, 30°; field of view, 26 cm; and matrix size, 256  $\times$  192 pixels. Section thickness varied according to brain size, ranging from 2.4 to 2.6 mm and covering the brain using a fixed number of 60 slices in each case. Acquisition time was 8 minutes 13 seconds. These series parameters produce anisotropic voxels with moderate spatial resolution (voxel dimensions, typically 1.0  $\times$  1.3  $\times$  2.5 mm) and an optimal signal-to-noise ratio, allowing reliable brain tissue segmentation.<sup>35,36</sup>

Imaging data were processed on an auxiliary workstation (Sun Ultra 5; Sun Microsystems Inc, Santa Clara, Calif) using a technical computing software program (MATLAB 5.3; The MathWorks Inc, Natick, Mass) and SPM software (SPM99; The Wellcome Department of Imaging Neuroscience, London, England).

All images were checked for artifacts, and the origin was placed on the anterior commissure before preparing MRIs for voxel-by-voxel analyses. In short, image preprocessing involved several automated procedures aimed at (1) optimally normalizing gray matter, white matter, and cerebrospinal fluid (CSF) segments using study and tissue-specific templates; (2) modulating voxel values from spatial normalization data to preserve volumetric information; and (3) averaging neighboring voxel values (smoothing) to load each element with region information. Each image transformation step is described in detail in the following subsections.

#### Template Creation

A template image was generated for each cranial compartment (gray matter, white matter, and CSF). Following the optimized voxel-based morphometry method proposed by Good et al,<sup>37</sup> each 3-dimensional MRI was firstly transformed to a standard stereotactic space by normalizing the imaging data to the SPM99 T<sub>1</sub> template. Next, each image was smoothed using an 8-mm full-width at half-maximum isotropic Gaussian kernel, and a mean image was created to serve as a whole-brain template in this study. All the structural images were then normalized to this study-specific template. Spatial normalization used the residual sum of squared differences as the matching criterion and involved a first step consisting of a 12-parameter affine transformation<sup>38</sup> and a second step consisting of nonlinear iterations using 7  $\times$  8  $\times$  7 basis functions accounting for global nonlinear shape differences.<sup>39</sup>

Normalized images were then segmented into gray matter, white matter, and CSF partitions. As is characteristic of SPM99 segmentations, each voxel was assigned a probability of belonging to a particular partition based on its signal intensity value and information from previous SPM99 probability maps describing the relative distribution of tissue types. In this step, an image intensity nonuniformity correction was performed.<sup>40</sup> These normalized and segmented images from the 144 study participants were finally smoothed using an 8-mm full-width at half-maximum isotropic Gaussian kernel and averaged to create gray matter, white matter, and CSF templates. These tissue-specific templates served to obtain optimal normalization parameters for each tissue type.

**Table 1. Clinical Characteristics of 72 Patients With OCD**

Characteristic	Value	Score		
		0 (Absent)	1 (Mild)	2 (Prominent)
Age at onset of OCD, mean ± SD (range), y	17.0 ± 5.9 (6-40)			
Duration of illness, mean ± SD (range), y	13.0 ± 10.5 (1-51)			
Y-BOCS score, mean ± SD (range)				
Global	26.7 ± 7.1 (7-38)			
Obsessions	13.7 ± 3.4 (6-19)			
Compulsions	13.0 ± 4.8 (0-19)			
OCD symptoms (Mataix-Cols et al <sup>25</sup> dimensions), No. (%) <sup>*</sup>				
Symmetry and ordering		50 (69.4)	12 (16.7)	10 (13.9)
Hoarding		56 (77.8)	11 (15.3)	5 (6.9)
Contamination and cleaning		41 (56.9)	14 (19.4)	17 (23.6)
Aggressive and checking		23 (31.9)	19 (26.4)	30 (41.7)
Sexual and religious obsessions		55 (76.4)	4 (5.6)	13 (18.1)
Comorbid diagnoses				
Significant history of depression, No. (%)	26 (36.1)			
HAM-D score at inclusion, mean ± SD (range)	12.7 ± 5.4 (2-26)			
Significant history of anxiety, No. (%)				
Panic disorder	4 (5.6)			
Social phobia	5 (6.9)			
Generalized anxiety disorder	5 (6.9)			
HAM-A score at inclusion, mean ± SD (range)	13.3 ± 6.6 (0-30)			
Treatment status				
Never treated, No. (%)	5 (6.9)			
Previous SRI trials completed, No. (%)				
1	19 (26.4)			
2	21 (29.2)			
≥3	27 (37.5)			
Cumulative SRI use, mean ± SD (range, median), mo	41.0 ± 62.5 (0-396, 24.0)			
Previous low-dose neuroleptic use, No. (%)	12 (16.7)			
Complete behavioral therapy protocol, No. (%)	41 (56.9)			
Previous treatment with experimental TMS, No. (%)	10 (13.9)			
Stable medication use at time of MRI, No. (%)				
Medication free (>4 wk)	18 (25.0)			
Clomipramine hydrochloride	25 (34.7)			
Fluoxetine or fluvoxamine maleate	13 (18.1)			
Phenelzine sulfate	2 (2.8)			
Clomipramine with fluoxetine	14 (19.4)			

Abbreviations: HAM-A, Hamilton Rating Scale for Anxiety; HAM-D, Hamilton Rating Scale for Depression; MRI, magnetic resonance imaging; OCD, obsessive-compulsive disorder; SRI, serotonin reuptake inhibitor; TMS, transcranial magnetic stimulation; Y-BOCS, Yale-Brown Obsessive-Compulsive Scale.

\*A score of 2 (prominent) was allowed for more than 1 dimension.

### Optimal Normalization and Segmentation

Structural images in native space (not normalized) were segmented into gray matter, white matter, and CSF compartments. During this process, a fully automated procedure<sup>37</sup> was applied to extract tissue of interest from nonbrain voxels (scalp, skull, or dural venous sinuses). Extracted images for each tissue type were normalized to their tissue-specific templates. The optimized normalization parameters obtained for each tissue compartment in this step were applied to the original whole-brain images. The resulting 3 models were resliced to a final voxel size of 1.5 mm<sup>3</sup>. Each optimally normalized tissue-specific whole-brain model was then segmented to isolate the corresponding tissue compartment. In this latter process, automated extraction of residual nonbrain voxels was again applied.

### Modulation

Spatial normalization inherently reduces size variations between different brains. To restore original volume information within each voxel, voxel values in the segmented images

were modulated (multiplied) by the Jacobian determinants derived from the spatial normalization step. The Jacobian determinant of a voxel is a numerical factor reflecting volume changes (expansions or contractions) occurring when an image from a subject is warped to match the template. If, for example, a brain structure has half the volume of that of the template, then its volume will be doubled during spatial normalization. In this case, modulation will restore original volume information by reducing voxel values to half. The analysis of modulated data, therefore, allows direct testing for regional differences in the absolute amount (volume) of each tissue type.<sup>37</sup>

### Smoothing

Finally, the images were smoothed using a 12-mm full-width at half-maximum isotropic Gaussian kernel. This operation conditions the data to conform more closely to the Gaussian field model underlying the statistical procedures used in regional analyses.<sup>41</sup> After smoothing, the intensity in each voxel is a locally weighted average of tissue volume from a region of voxels defined by the size of the smoothing kernel.<sup>40</sup>

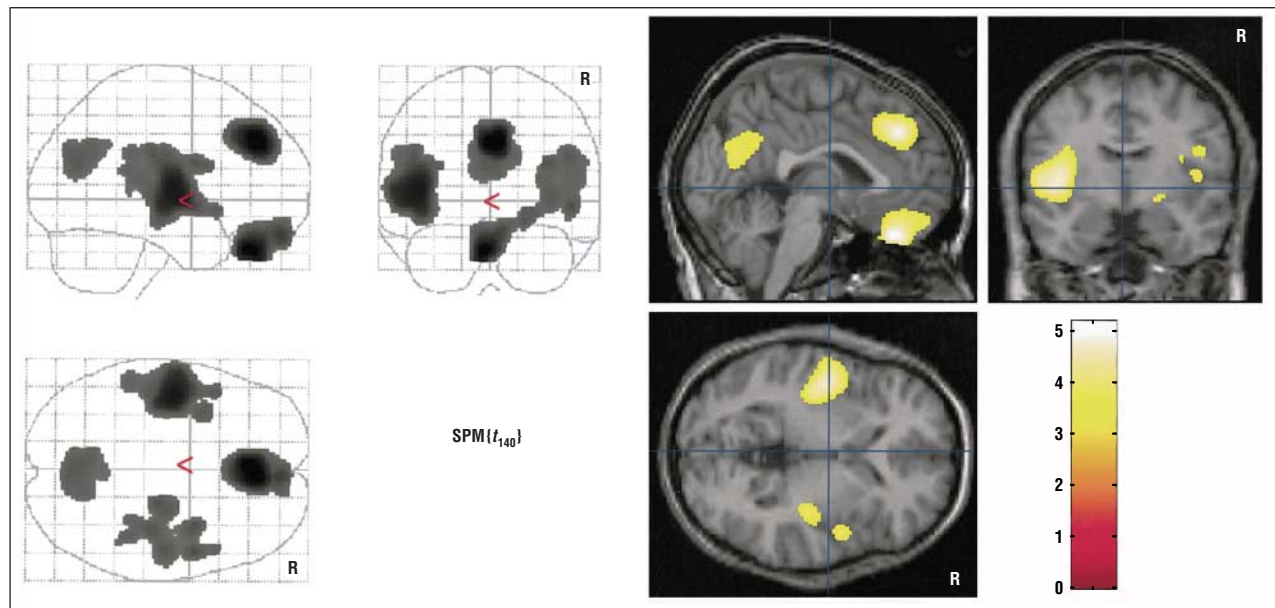


**Figure 1.** Statistical parametric  $t$  map ( $SPM\{t_{140}\}$ ) of gray matter volume reduction in obsessive-compulsive disorder. Clusters of more than 1000 voxels showing uncorrected  $P < .001$  are displayed. The 3 orthogonal planes on the left side represent a typical maximum intensity projection "glass brain," and the set of images on the right side illustrate results superimposed on normalized structural images in selected planes. R indicates the right hemisphere, and the color bar represents the  $t$  score. Significant voxels were found in the orbitofrontal cortex, medial frontal gyrus, and left insulo-opercular region (corrected  $P < .05$ ). Note that right insular and retrosplenial changes, showing a tendency toward significance, are also displayed.

### Process Overview

The result of the whole process is that global brain shape variability is removed by spatial normalization, and different brains, adjusted to the same stereotactic space, can be compared voxel by voxel. The comparison is sensitive to volumetric differences in brain structures, as each voxel value is adjusted for volume changes occurring in the normalization step (modulation). Therefore, a voxel value difference between 2 subject groups at a specific brain coordinate means that the 2 populations differ in brain volume at this location (and at its surrounding tissue, as the data are finally smoothed). The accuracy in measuring volume changes is determined by precision of spatial normalization that is typically less optimal for smaller structures in voxel-based morphometry. Spatial smoothing helps compensate for inexact normalization. A detailed explanation of what modulated voxel-based morphometry measures and its inherent limitations is reported elsewhere.<sup>42</sup>

### STATISTICAL ANALYSIS

Global brain volume measurements (obtained from the non-normalized images) were compared in patients and control subjects using the independent samples  $t$  test.

The SPM99 tools were used to map regionally specific volume differences throughout the brain on a voxel-by-voxel basis. Comparisons between groups were conducted separately for each tissue type. Data expressing absolute voxel values and data normalized for global differences in voxel intensity across scans were analyzed. A proportional scaling method was used to scale each voxel value to a grand mean of 100. Each group comparison generated 2  $t$  statistic maps ( $SPM\{t\}$ ) corresponding to 2 opposite contrasts: volume decrease and increase, displayed at a threshold of  $P < .001$ . Regional differences were reported to be significant at  $P < .05$  after correction for multiple comparisons. Age was introduced as a regressor (covariate) in the comparisons between patients and control subjects. Pearson correlations and partial correlations were used in the regional and clinical analyses. A pos-

sible interaction between age and group was specifically investigated by comparing age-tissue volume correlations between patients and control subjects. Spatial coordinates from all the obtained maps were converted to standard Talairach coordinates<sup>43</sup> using a nonlinear transform of SPM99 standard space to Talairach space.<sup>44</sup>

## RESULTS

### GLOBAL VOLUME MEASUREMENTS

Mean  $\pm$  SD intracranial volume was similar in patients with OCD and control subjects ( $1407 \pm 167$  and  $1412 \pm 145$  mL, respectively;  $t_{142} = -0.2$ ;  $P = .86$ ). Patients showed a tendency toward smaller gray matter volumes, with a mean difference of 24 mL (mean  $\pm$  SD,  $739 \pm 82$  mL in patients and  $763 \pm 78$  mL in controls;  $t_{142} = -1.8$ ;  $P = .07$ ).

### GRAY MATTER, WHITE MATTER, AND CSF VOXEL-BASED ANALYSES

Compared with control subjects, patients with OCD showed significant absolute decreases in gray matter volume in the medial frontal gyrus (involving the anterior paracingulate cortex), the medial aspect of the orbitofrontal cortex, and the left insulo-opercular region (Figure 1). The posterior paracingulate cortex (at the precuneus-cuneus junction) and the insulo-opercular region of the right hemisphere showed a tendency for gray matter reduction, but differences in these regions were not statistically significant after correcting for multiple comparisons.

No regions in patients with OCD showed absolute increases in gray matter volume. Statistically significant increases, however, were observed after normalizing the data to global gray matter content. We observed relative increases in gray matter volume bilaterally in the ven-

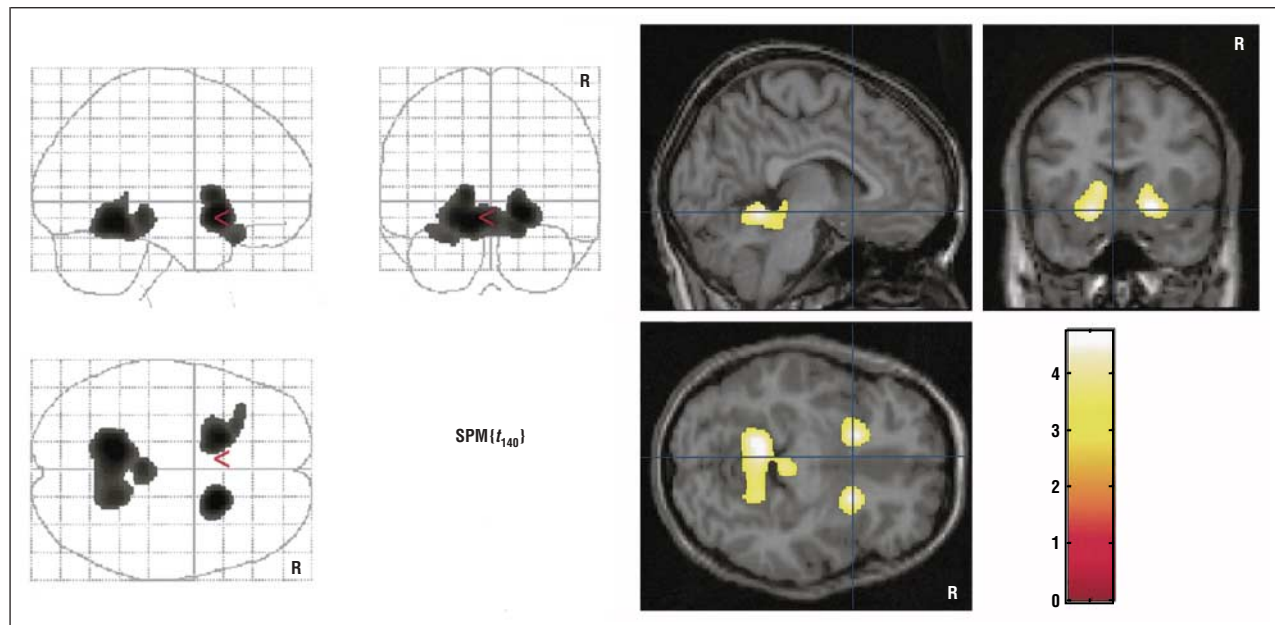


**Figure 2.** Statistical parametric  $t$  map ( $SPM\{t_{140}\}$ ) showing relative increases in gray matter volume in obsessive-compulsive disorder. Clusters of more than 1000 voxels at  $P < .001$  are displayed. R indicates the right hemisphere, and the color bar represents the  $t$  score. Significant voxels were found in the ventral part of the striatum, including the ventral striatum proper area, and in the anterior cerebellum (corrected  $P < .05$ ).

tral part of the striatum, including the ventral aspect of the putamen and the area of the ventral striatum proper (nucleus accumbens and olfactory tubercle), and in the anterior cerebellum (anterior lobule of the cerebellar vermis and part of the left anterior cerebellar hemisphere) (**Figure 2**).

**Figure 3** shows gray matter volume decreases and increases in 11 representative sagittal views. These images summarize and expand the description of our main results by mapping the distribution of the observed OCD brain changes more comprehensively.

No region was found to show statistically significant white matter decreases or increases in patients with OCD compared with controls.

No region in the CSF spaces showed statistically significant volume reductions. Patients, however, did show volume increases involving the medial orbitofrontal and left perisylvian CSF spaces. This CSF pattern broadly matched the gray matter findings, as CSF increases were adjacent to the regions showing statistically significant gray matter volume decreases. For left perisylvian CSF spaces, however, the observed changes were somewhat more anteriorly located (**Table 2**).

Table 2 reports significant peak differences in voxel volumes observed between patients with OCD and control subjects. Each peak corresponds to the voxel showing the most significant difference, although the changes do not refer exclusively to the reported coordinates. Each voxel receives a weighted effect of a voxel region showing a 12-mm diameter (at full-width at half-maximum).

All comparisons were repeated with slice thickness in the regression as a covariate to exclude a possible confounding effect of slice thickness variations across participants. The reported results did not change after this analysis.

## INTERREGIONAL CORRELATIONS

We investigated whether volume variations in the regions differing between patients with OCD and controls were related to each other. A correlation analysis was performed using the voxel values corresponding to the 6 peak coordinates identified in the gray matter analysis (**Table 3**). A definite pattern of correlations was observed in patients showing a significant inverse correlation between the subcortical (right and left striatal regions) and cortical (medial frontal, orbitofrontal, and insulo-opercular) structures. In addition, positive correlations were found between cortical regions and between right and left striatal areas. In the control group, this pattern was not found, and the only significant finding corresponded to a positive correlation between the striatal areas.

We also investigated whether volume variations in the regions of interest correlated with other parts of the OCD brain. Separate voxel-based brain maps were performed for the 6 gray matter regions using the peak coordinate value of each region as a predictor variable. Few findings were obtained in this analysis. The right striatal region positively correlated with a bilateral area involving the posterior cingulate cortex (peak at Talairach  $x, y, z: 7, -44, 15$  mm;  $r = 0.53$ ,  $t_{69} = 5.2$ ; corrected  $P = .01$ ) and inversely correlated with a diencephalic area that included part of the medial and anterior thalamus bilaterally (peak at Talairach  $x, y, z: 0, -3, 3$  mm;  $r = -0.54$ ,  $t_{69} = 5.4$ ; corrected  $P = .008$ ).

In a post hoc analysis, we tested whether volume increases or decreases occurred in the OCD posterior cingulate and thalamus at lower significance thresholds. We did not find any difference between patients and control subjects in this analysis.

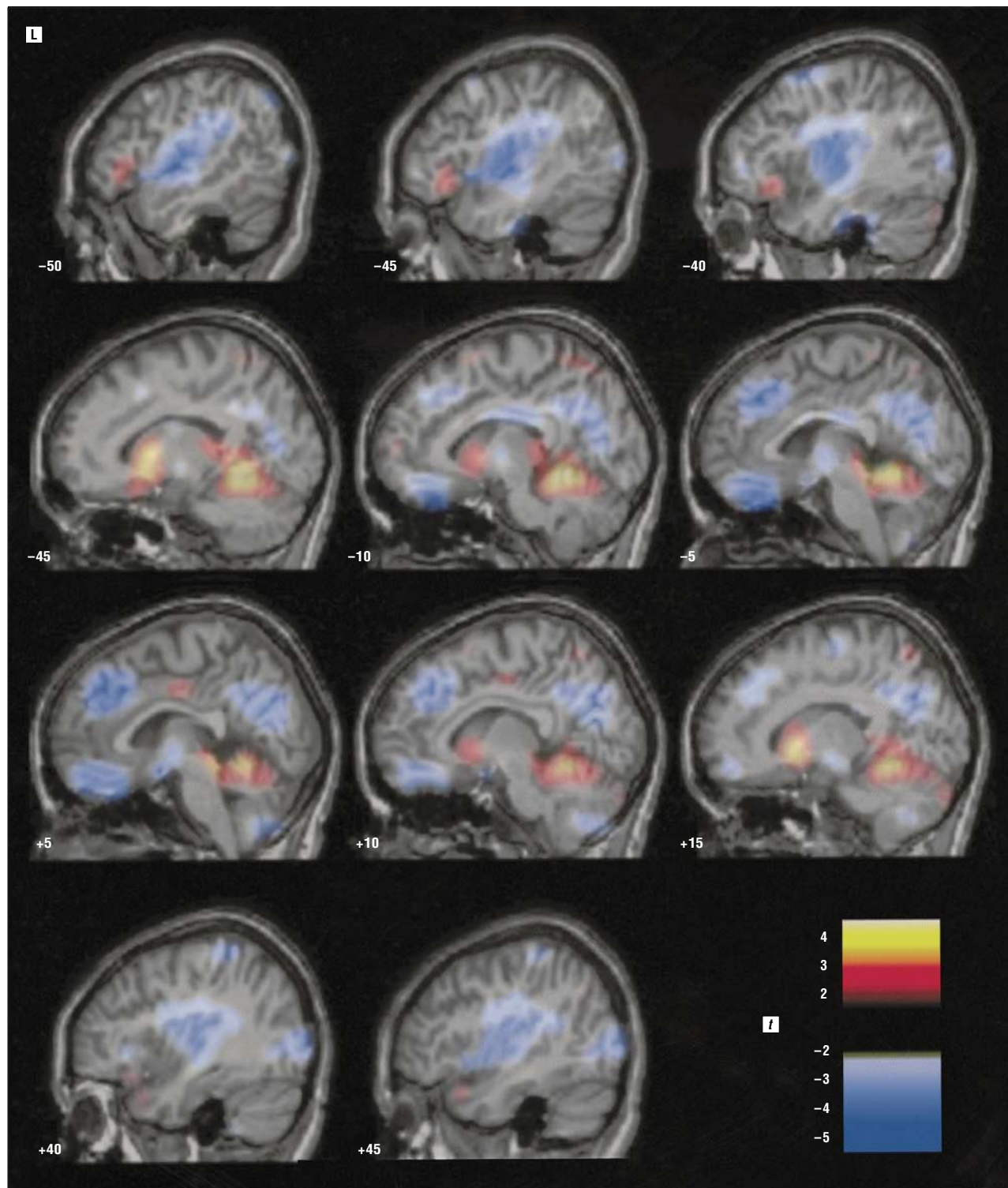


**Figure 3.** Summary and extended illustration of gray matter findings. The maps of decreases (cold colors) and relative increases (hot colors) of gray matter volume in obsessive-compulsive disorder are superimposed on representative sagittal views. Voxels showing  $t$  values greater than 2 or less than  $-2$  are displayed. L indicates the left hemisphere, and  $t$  refers to the statistic. Numbers at the bottom of each slice represent the Talairach "x" coordinate in millimeters. This composition allows us to accurately appreciate the anatomy of each observed change.

#### CORRELATION OF CLINICAL VARIABLES WITH OCD BRAIN ANATOMY

We observed a different effect of age on tissue volume for both study groups (**Table 4** and **Figure 4**). Patients with OCD showed a preservation (absence of

age-related volume decrease) of the ventral striatum areas bilaterally, although the effect was particularly relevant for the right side (age  $\times$  group interaction was significant at Talairach  $x, y, z: 21, 6, -4$  mm;  $t_{140}=5.41$ ; corrected  $P=.001$ ). In contrast, the effect of age on the cortical regions was similar for patients and control sub-

**Table 2. Regional Volume Differences Between Patients With Obsessive-Compulsive Disorder and Control Subjects**

Peak Coordinates, mm*			<i>t</i> <sub>140</sub>	P Value†	Anatomical Location
x	y	z			
<b>Absolute Decrease in Gray Matter</b>					
3	39	30	5.17	.004	Right medial frontal gyrus
-3	32	-27	4.97	.008	Left gyrus rectus
-45	-9	5	4.75	.02	Left posterior insula
<b>Relative Increase in Gray Matter</b>					
19	13	-7	4.75	.01	Right ventral putamen
-12	-47	-8	4.69	.02	Left anterior cerebellum
-19	14	-10	4.45	.04	Left ventral putamen
<b>Absolute Increase in Cerebrospinal Fluid Spaces</b>					
6	56	-22	4.76	.001	Interhemispheric space
1	37	-27	4.69	.01	Interhemispheric space
-45	22	-2	4.35	.04	Left frontotemporal space
-58	21	-9	4.30	.045	Left frontotemporal space

\*Coordinates (x, y, z) refer to the standard stereotactic space defined by Talairach and Tournoux.<sup>43</sup>

†Corrected for multiple comparisons throughout the brain.

**Table 3. Pattern of Regional Correlations for Representative Voxels\***

	<i>r</i> (P Value)†				
	Medial Frontal	Orbitofrontal	Insulo-opercular	Right Striatum	Left Striatum
Patients (n = 72)					
Orbitofrontal	0.54 (<.001)‡				
Insulo-opercular	0.42 (<.001)‡	0.20 (.09)			
Right striatum	-0.52 (<.001)‡	-0.35 (.003)‡	-0.38 (.001)‡		
Left striatum	-0.39 (.001)‡	-0.28 (.02)	-0.35 (.003)‡	0.72 (<.001)‡	
Anterior cerebellum	-0.22 (.06)	-0.07 (.56)	-0.12 (.34)	0.32 (.007)	0.29 (.02)
Controls (n = 72)					
Orbitofrontal	0.30 (.01)				
Insulo-opercular	0.18 (.12)	0.02 (.89)			
Right striatum	-0.00 (.97)	0.02 (.90)	0.14 (.26)		
Left striatum	0.11 (.36)	0.02 (.89)	0.09 (.48)	0.54 (<.001)‡	
Anterior cerebellum	-0.01 (.97)	-0.05 (.69)	-0.01 (.96)	0.08 (.50)	0.34 (.004)

\*Adjusted to total gray matter volume using partial correlations.

†Two-tailed.

‡Significant after Bonferroni correction.

**Table 4. Correlations of Age With Volume Measurements at Peak Coordinates\***

	<i>r</i> (P Value)†					
	Medial Frontal	Orbitofrontal	Insulo-opercular	Right Striatum	Left Striatum	Anterior Cerebellum
Patients (n = 72)						
Age						
Pearson correlation	-0.57 (<.001)	-0.53 (<.001)	-0.47 (<.001)	0.07 (.54)	0.03 (.84)	0.10 (.41)
Partial correlation	-0.46 (<.001)	-0.42 (<.001)	-0.28 (.02)	0.61 (<.001)	0.41 (<.001)	0.34 (.004)
Controls (n = 72)						
Age						
Pearson correlation	-0.60 (<.001)	-0.39 (.001)	-0.52 (<.001)	-0.40 (.001)	-0.33 (.005)	-0.05 (.68)
Partial correlation	-0.48 (<.001)	-0.16 (.18)	-0.28 (.02)	-0.02 (.75)	0.05 (.65)	0.21 (.08)

\*Total gray matter volume was used in partial correlations.

†Two-tailed.

jects. In both groups, gray matter volume decreased with age at a comparable rate. Age-related reduction of gray matter was a general effect in the brain. The correlation

of age with the total gray matter volume was  $r = -0.41$  in patients with OCD and  $r = -0.48$  in control subjects ( $P < .001$  for both).

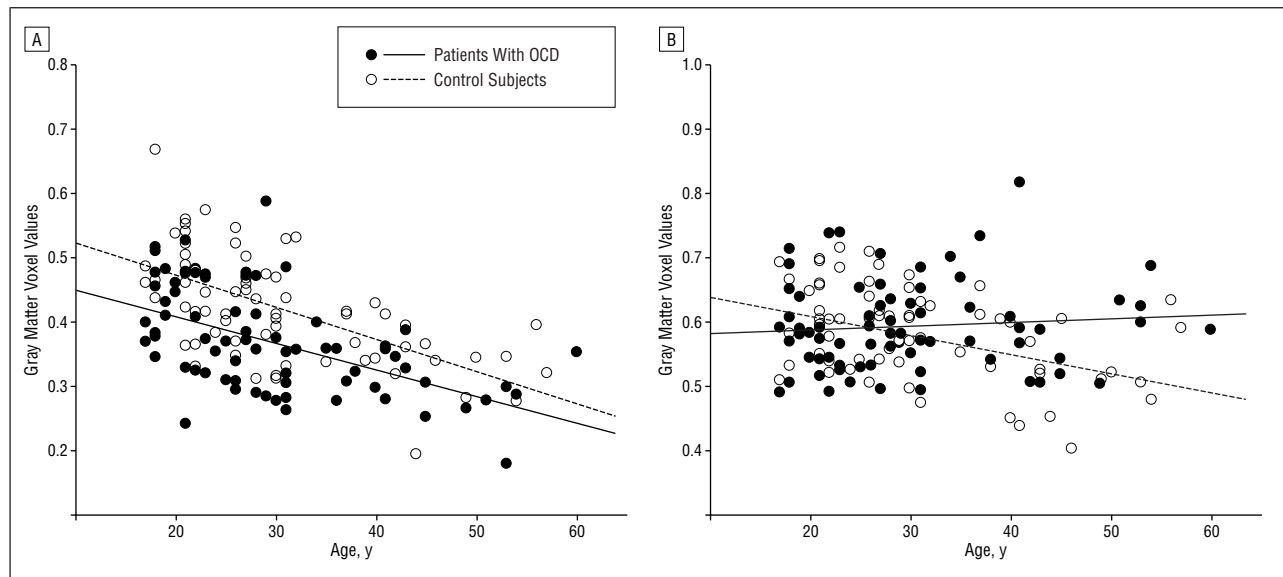


**Figure 4.** Age effect on obsessive-compulsive disorder (OCD) brain alterations in 2 representative areas at peak coordinates. A, In the medial frontal region, a similar age-related volume reduction is observed in patients with OCD and control subjects. B, In the right ventral striatum area, gray matter volume does not decrease with age in patients with OCD.

Illness duration effects were comparable to those observed for age. We found, for example, that this variable correlated inversely with total gray matter volume ( $r = -0.48$ ;  $P < .001$ ) and with normalized right striatal area ( $r = 0.50$ ;  $P < .001$ ). Age and illness duration were strongly related in this OCD sample ( $r = 0.84$ ;  $P < .001$ ). No significant effect was observed when the age of patients at the onset of OCD was analyzed.

Separate voxel-based analyses were conducted for sex, disease severity (Yale-Brown Obsessive-Compulsive Scale scores), comorbid anxiety and depression symptoms (Hamilton scores), treatment type (including medication and behavioral therapy, current and past history), number of treatments received, and total treatment duration. In no case did these variables significantly predict anatomical changes in the OCD brain.

#### ANALYSIS FOR SEPARATE SYMPTOM DIMENSIONS

Scores on the 5 defined symptom dimensions were used as predictors in further analyses attempting to map brain changes associated with a given factor. We found no significant correlation between these scores and the values of voxels included in the abnormal regions. Similarly, we found no significant difference for these regions when comparing patients with symptoms for a given dimension with the rest of the sample.

We made one relevant finding when the voxel-based maps obtained in this analysis were checked to identify possible changes in other brain areas. Patients with “prominent” aggressive obsessions and checking compulsions (factor 4) showed a relative decrease in gray matter volume in the right amygdala region compared with the rest of the OCD sample (**Figure 5**). Differences at peak coordinates (Talairach  $x, y, z$ : 18, -9, -13 mm) were significant ( $t_{60} = 5.3$ ; corrected  $P = .01$ ), adjusted to brain volume, age, and sex. These 30 patients also showed a

smaller right amygdala region than their 30 matched control subjects in relative and absolute terms ( $t_{120} = 5.8$ ; corrected  $P < .001$ , adjusted to brain volume;  $t_{126} = 4.5$ ; corrected  $P = .04$ , for nonadjusted comparison). The rest of the sample, however, did not differ from their control counterparts.

#### COMMENT

Voxel-based mapping of structural brain alterations in patients with OCD revealed statistically significant reductions of gray matter volume in the medial frontal and orbitofrontal cortices and in the left insulo-opercular region and a relative volume increase in the ventral part of the striatum and anterior cerebellum. Cortical and subcortical changes were abnormally coupled in OCD, and age statistically significantly contributed to the relative enlargement in the ventral striatum area. The clinical expression of OCD was not related to these anatomical changes, although patients with aggressive obsessions and checking compulsions showed a reduced right amygdala volume.

Early imaging studies typically evaluated selected cerebral regions in few patients and provided notably heterogeneous results.<sup>8</sup> More recently, Jenike et al<sup>21</sup> used 3-dimensional MRI and parceled the entire brain in several regions of interest. They suggested that structural brain alterations in OCD may be widely distributed. Kim et al<sup>22</sup> assessed the OCD brain using voxel-based means and analyzed MRI studies of 25 patients with no correction for multiple comparisons. They identified brain regions showing altered gray matter “density” (direct volume testing was not possible until recent technical improvements) and found alterations distributed over multiple areas of the 4 cerebral lobes and diencephalon. Their results only marginally coincide with our data, but both studies may be considered complementary.

In keeping with the increasing interest in the comprehensive assessment of OCD brain anatomy, we used

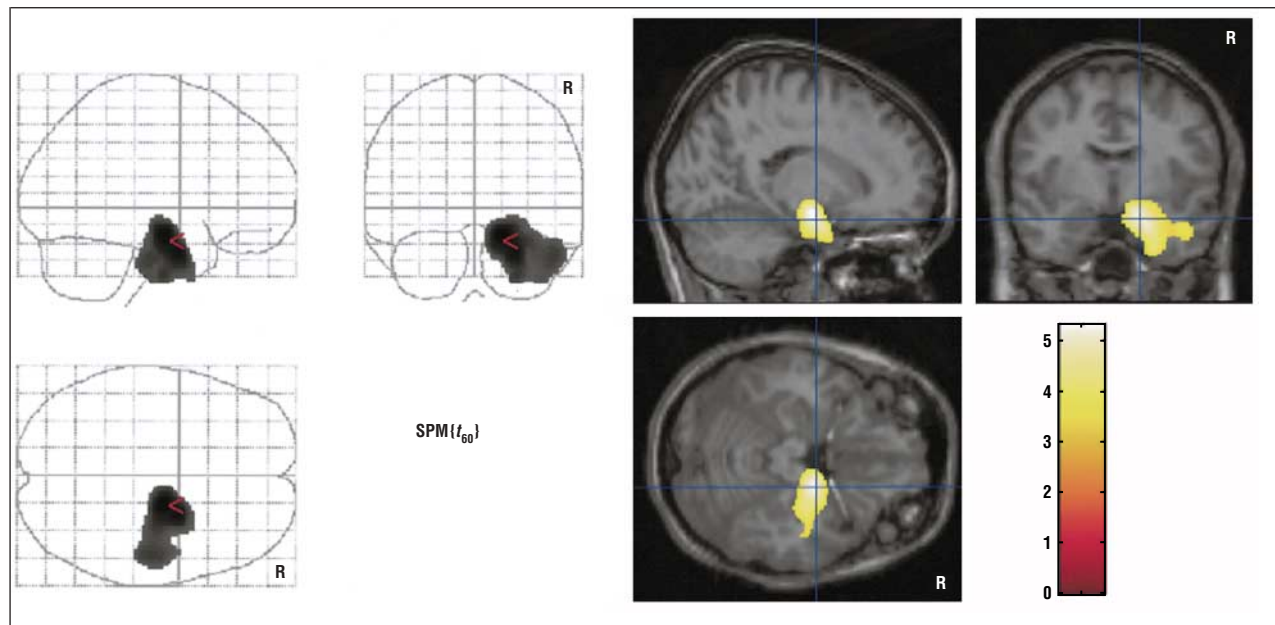


**Figure 5.** Statistical parametric  $t$  map ( $SPM\{t_{60}\}$ ) of relative gray matter volume reduction in patients with prominent aggressive obsessions and checking compulsions compared with the rest of the obsessive-compulsive disorder sample (voxel display,  $P < .001$ ). R indicates the right hemisphere, and the color bar represents the  $t$  score. Significant voxels were found in a right hemisphere region involving the amygdala (corrected  $P < .05$ ).

highly automated voxel-based morphometric procedures and examined the entire cerebral parenchyma in a large number of patients (the largest structural MRI study to date in OCD). We adopted an improved method for modulating data that allowed direct volume measurements. In our analysis, voxel values specifically expressed variations in the absolute amount of brain tissue, in contrast with previous voxel-based studies in which the interpretation of results was not self-evident, as voxel values expressed variations in structure shape and tissue composition.

These study characteristics may well improve the probability of capturing the more prevalent structural alterations in OCD. Moreover, some relevant features of the OCD brain may probably be detected on a voxelwise basis only. Indeed, structural changes in patients do not exactly match specific cerebral nuclei or definite gyri but instead involve divisions of anatomical structures. This finding may in part explain the difficulty in identifying structural brain alterations in the studies that used anatomical boundaries to delimit the regions of interest.<sup>8</sup> Nevertheless, voxel-based morphometry is still limited in that brain normalization and severe smoothing may cause information loss and degrade anatomical details in small structures. In addition, there is a real need to ascertain to what extent the results obtained with volume-modulated voxel-based approaches are comparable to those of conventional morphometry. We would, however, point out that the studies conducted in large samples in other neuropsychiatric populations suggest that standard and voxel-based methods produce compatible findings.<sup>45</sup>

The proposed models of OCD symptom mediation generally coincide in that brain dysfunction does not involve the entire frontosubcortical system but rather the ventral striatum and functionally related orbitofrontal and cingulate cortices specifically.<sup>2,7,8,46-49</sup> We detected alter-

ations in the ventral part of the striatum and the medial (orbital and paracingulate) aspect of the frontal lobes. Thus, it seems that alterations in the “limbic” component of the frontosubcortical system may also be observed in the structural domain. It is relevant, however, that we found volume reduction in the cortex and relative expansion of tissue at the subcortical level, whereas in the functional studies,<sup>7-9</sup> both levels seem hyperactive.

Our interregional correlation analysis revealed that cortical and striatal alterations are coupled in OCD. The observed inverse correlation between the 2 brain levels is pathologic as it was not present in control subjects. Such an analysis may indicate that the whole pattern of alterations detected in the study reflects a global disorder in a large-scale system as opposed to a simple sum of isolated changes. Baxter et al<sup>48</sup> also found abnormal frontosubcortical correlations in OCD in their early positron emission tomographic assessment. The correlation disappeared with symptom improvement in their treatment-responsive patients.

Prevailing hypotheses for the pathogenesis of OCD propose that a defective,<sup>48</sup> imbalanced,<sup>7</sup> hypertonic<sup>47</sup> striatum originates OCD symptoms by disturbing the frontosubcortical balance in the striatal loops. Our age analysis may provide evidence for the dynamic nature of the striatal disturbance, as it suggests that subcortical alterations progress throughout the age period studied. In this context, structural changes in the striatum could be the anatomical expression of enduring striatal dysfunction. Age did not contribute to the occurrence of OCD cortical alterations. In both study groups, cortical gray matter volume decreased with age at a comparable rate. Therefore, early structural changes and changes developing during the illness may coexist in OCD.

The frontostriatal system serves to modulate behavioral responses and works together with other brain sys-

tems, such as the cerebellum.<sup>50</sup> The cerebellar hemispheres affect fine motor and cognitive responses, whereas the medial rostral cerebellum affects arousal, autonomic behavior, and emotional responsiveness.<sup>51,52</sup> The anterior vermis and the associated fastigial nucleus are considered to be the “limbic cerebellum,” which is directly connected to the ventral tegmental area that provides dopamine to the ventral striatum and facilitates neural activity in the septal region (reviewed by Schmahmann<sup>52</sup>). We found relative gray matter volume increases in the ventral part of the striatum and in the functionally related rostral cerebellum. This finding may suggest cerebellar involvement in the pathogenesis of OCD.

At first sight, the changes observed in the left posterior insula and adjacent opercular tissue may seem difficult to harmonize with the other alterations. This region of the brain has traditionally been related to language operations, but recent studies have provided a wealth of data suggesting a key role in the perception of the body scheme, mediation of pain responses, visceral awareness, and evaluation of the affective components of sensory information.<sup>53</sup> We do not know the intrinsic mechanisms that may functionally link the insulo-opercular changes to the alterations occurring in the frontostriatal system in OCD. Anatomically, however, the relationship is direct, as the frontoparietal operculum and the insula send strong connections to the ventral part of the striatum.<sup>54,55</sup>

The operculo-insular system processes sensory inflow before reaching the amygdala.<sup>53,56</sup> Therefore, in this context, the amygdala (a third party in the genesis of compulsions<sup>49</sup>) is doubly prone to hyperactivation in OCD, from reduction of the inhibitory tone provided by an altered orbitofrontal cortex as proposed by Rauch et al<sup>49</sup> and from an excessive input of deficiently filtered sensory stimulation as a result of a “weak” operculo-insular system. In tune with this amygdalocentric perspective, we found that aggressive obsessions and checking compulsions, a dimension involving OCD behavior openly related to fear, were associated with a smaller right amygdala area. Szeszko et al<sup>20</sup> previously reported reduced right amygdala size in OCD, although their finding was not ascribed to a particular clinical subtype.

We attempted to link the observed findings with the core of the OCD phenomenon. Nevertheless, we should alternatively consider treatment as a potential contributor to regional brain size variations. Volume increases in basal ganglia have been reported as a consequence of prolonged neuroleptic administration,<sup>57</sup> and, furthermore, increased thalamic volume was observed in medication-free patients<sup>15,22</sup> normalizing with paroxetine monotherapy.<sup>15</sup> Although we found no association between the administered treatments and brain changes present in our patients, medication could be responsible for obtaining negative findings for the thalamus. It is possible in this study, as in others,<sup>21</sup> that active treatment at the time of imaging prevented us from obtaining the increased thalamic volume reported for medication-free patients. Another possible study limitation is that 10 patients had received experimental treatment with transcranial magnetic stimulation and that the long-term neural consequences of such treatment are poorly understood.

Although we found structural alterations in brain systems metabolically altered in OCD, there is no complete anatomical coincidence between our results and functional data. Hypermetabolism in positron emission tomographic studies is also observed in more lateral aspects of the orbitofrontal cortex and in more medial aspects of the ventral striatum.<sup>9</sup> Part of such a discordance could perhaps be explained by technical arguments, but it is also feasible that functional and structural approaches emphasize, in part, different aspects of the disorder. Our data may complement functional studies mainly by further delimiting the anatomy of changes, by showing that either decreases or increases in tissue volume are compatible with hypermetabolism, and by suggesting that brain alterations in OCD may progressively vary during the disease.

Submitted for publication June 3, 2003; final revision received January 21, 2004; accepted January 29, 2004.

This study was supported in part by grants 00/0226 and PI020102 from the Fondo de Investigación Sanitaria, Madrid, Spain; by the Fundació La Marató TV3, Barcelona; and by grants 1999SGR-328 and 2000XT-43 from the Direcció General de Recerca de la Generalitat de Catalunya, Barcelona.

We thank Gerald Fannon, PhD, for revising the manuscript.

Correspondence: Jesús Pujol, MD, Magnetic Resonance Center of Pedralbes, J Anselm Clavé 100, Esplugues de Llobregat, Barcelona 08950, Spain (jpujol@cetir.es).

## REFERENCES

- McGuire PK. The brain in obsessive-compulsive disorder. *J Neurol Neurosurg Psychiatry*. 1995;59:457-459.
- Insel TR. Toward a neuroanatomy of obsessive-compulsive disorder. *Arch Gen Psychiatry*. 1992;49:739-744.
- Laplante D, Levasseur M, Pillon B, Dubois B, Baulac M, Mazoyer B, Tran Dinh S, Sette G, Danze F, Baron JC. Obsessive-compulsive and other behavioural changes with bilateral basal ganglia lesions: a neuropsychological, magnetic resonance imaging and positron tomography study. *Brain*. 1989;112:699-725.
- Berthier ML, Kulisevsky J, Gironell A, Heras JA. Obsessive-compulsive disorder associated with brain lesions: clinical phenomenology, cognitive function, and anatomic correlates. *Neurology*. 1996;47:353-361.
- Savage CR. Neuropsychology of obsessive-compulsive disorder: research findings and treatment implications. In: Jenike MA, Baer L, Minichiello WE, eds. *Obsessive-compulsive Disorder: Practical Management*. St Louis, Mo: Mosby-Year Book Inc; 1998:254-275.
- Greenberg BD, Murphy DL, Rasmussen SA. Neuroanatomically based approaches to obsessive-compulsive disorder: neurosurgery and transcranial magnetic stimulation. *Psychiatr Clin North Am*. 2000;23:671-686.
- Saxena S, Rauch SL. Functional neuroimaging and the neuroanatomy of obsessive-compulsive disorder. *Psychiatr Clin North Am*. 2000;23:563-586.
- Saxena S, Brody AL, Schwartz JM, Baxter LR. Neuroimaging and fronto-subcortical circuitry in obsessive-compulsive disorder. *Br J Psychiatry Suppl*. 1998;35:26-37.
- Rauch SL, Baxter LR Jr. Neuroimaging in obsessive-compulsive disorder and related disorders. In: Jenike MA, Baer L, Minichiello WE, eds. *Obsessive-compulsive Disorder: Practical Management*. St Louis, Mo: Mosby-Year Book Inc; 1998:289-317.
- Rosenberg DR, Keshavan MS, O'Hearn KM, Dick EL, Bagwell WW, Seymour AB, Montrose DM, Pierri JN, Birmaher B. Frontostriatal measurement in treatment-naive children with obsessive-compulsive disorder. *Arch Gen Psychiatry*. 1997;54:824-830.
- Luxenberg JS, Swedo SE, Flament MF, Friedland RP, Rapoport J, Rapoport SI. Neuroanatomical abnormalities in obsessive-compulsive disorder detected with quantitative X-ray computed tomography. *Am J Psychiatry*. 1988;145:1089-1093.

12. Robinson D, Wu H, Munne RA, Ashtari M, Alvir JM, Lerner G, Korean A, Cole K, Bogerts B. Reduced caudate nucleus volume in obsessive-compulsive disorder. *Arch Gen Psychiatry*. 1995;52:393-398.
13. Scarone S, Colombo C, Livian S, Abbruzzese M, Ronchi P, Locatelli M, Scotti G, Smeraldi E. Increased right caudate nucleus size in obsessive-compulsive disorder: detection with magnetic resonance imaging. *Psychiatry Res*. 1992;45:115-121.
14. Giedd JM, Rapoport JL, Garvey MA, Perlmutter S, Swedo SE. MRI assessment of children with obsessive-compulsive disorder or tics associated with streptococcal infection. *Am J Psychiatry*. 2000;157:281-283.
15. Gilbert AR, Moore GJ, Keshavan MS, Paulson LA, Narula V, Mac Master FP, Stewart CM, Rosenberg DR. Decrease in thalamic volumes of pediatric patients with obsessive-compulsive disorder who are taking paroxetine. *Arch Gen Psychiatry*. 2000;57:449-456.
16. Kellner CH, Jolley RR, Holgate RC, Austin L, Lydiard RB, Laraia M, Ballenger JC. Brain MRI in obsessive-compulsive disorder. *Psychiatry Res*. 1991;36:45-49.
17. Aylward EH, Harris GJ, Hoehn-Saric R, Barta PE, Machlin SR, Pearlson GD. Normal caudate nucleus in obsessive-compulsive disorder assessed by quantitative neuroimaging. *Arch Gen Psychiatry*. 1996;53:577-584.
18. Stein DJ, Coetzer R, Lee M, Davids B, Bouwer C. Magnetic resonance brain imaging in women with obsessive-compulsive disorder and trichotillomania. *Psychiatry Res*. 1997;74:177-182.
19. Bartha R, Stein MB, Williamson PC, Drost DJ, Neufeld RW, Carr TJ, Canaran G, Densmore M, Anderson G, Siddiqui AR. A short echo <sup>1</sup>H spectroscopy and volumetric MRI study of the corpus striatum in patients with obsessive-compulsive disorder and comparison subjects. *Am J Psychiatry*. 1998;155:1584-1591.
20. Szeszko PR, Robinson D, Alvir JM, Bilder RM, Lencz T, Ashtari M, Wu H, Bogerts B. Orbital frontal and amygdala volume reductions in obsessive-compulsive disorder. *Arch Gen Psychiatry*. 1999;56:913-919.
21. Jenike MA, Breiter HC, Baer L, Kennedy DN, Savage CR, Olivares MJ, O'Sullivan RL, Shera DM, Rauch SL, Keuthen N, Rosen BR, Caviness VS, Filipek PA. Cerebral structural abnormalities in obsessive-compulsive disorder: a quantitative morphometric magnetic resonance imaging study. *Arch Gen Psychiatry*. 1996;53:625-632.
22. Kim JJ, Lee MC, Kim J, Kim IY, Kim SI, Han MH, Chang KH, Kwon JS. Grey matter abnormalities in obsessive-compulsive disorder: statistical parametric mapping of segmented magnetic resonance images. *Br J Psychiatry*. 2001;179:330-334.
23. First MB, Spitzer RL, Gibbon M, Williams JBW. *Structured Clinical Interview for DSM-IV Axis I Disorders—Clinician Version (SCID-CV)*. Washington, DC: American Psychiatric Press; 1997.
24. Oldfield RC. The assessment and analysis of handedness: the Edinburgh Inventory. *Neuropsychologia*. 1971;9:97-113.
25. Mataix-Cols D, Rauch SL, Manzo PA, Jenike MA, Baer L. Use of factor-analyzed symptom dimensions to predict outcome with serotonin reuptake inhibitors and placebo in the treatment of obsessive-compulsive disorder. *Am J Psychiatry*. 1999;156:1409-1416.
26. Goodman WK, Price LH, Rasmussen SA, Mazure C, Fleischmann RL, Hill CL, Heninger GR, Charney DS. The Yale-Brown Obsessive Compulsive Scale. I: development, use, and reliability. *Arch Gen Psychiatry*. 1989;46:1006-1011.
27. Baer L. Factor analysis of symptom subtypes of obsessive compulsive disorder and their relation to personality and tic disorders. *J Clin Psychiatry*. 1994;55 (suppl):18-23.
28. Leckman JF, Grice DE, Boardman J, Zhang H, Vitale A, Bondi C, Alsobrook J, Peterson BS, Cohen DJ, Rasmussen SA, Goodman WK, McDougle CJ, Pauls DL. Symptoms of obsessive-compulsive disorder. *Am J Psychiatry*. 1997;154:911-917.
29. Rauch SL, Dougherty DD, Shin LM, Alpert NM, Manzo P, Leahy L, Fischman AJ, Jenike MA, Baer L. Neural correlates of factor-analyzed OCD symptom dimensions: a PET study. *CNS Spectr*. 1998;3:37-43.
30. Mataix-Cols D, Baer L, Rauch SL, Jenike MA. Relation of factor-analyzed symptom dimensions of obsessive-compulsive disorder to personality disorders. *Acta Psychiatr Scand*. 2000;102:199-202.
31. Hamilton M. A rating scale for depression. *J Neurol Neurosurg Psychiatry*. 1960;23:56-62.
32. Hamilton M. The assessment of anxiety state by rating. *Br J Med Psychol*. 1959;32:50-55.
33. Alonso P, Pujol J, Cardoner N, Benlloch L, Deus J, Menchon JM, Capdevila A, Vallejo J. Right prefrontal repetitive transcranial magnetic stimulation in obsessive-compulsive disorder: a double-blind, placebo-controlled study. *Am J Psychiatry*. 2001;158:1143-1145.
34. Shtasel DL, Gur RE, Mozley PD, Richards J, Taleff MM, Heimberg C, Gallacher F, Gur RC. Volunteers for biomedical research: recruitment and screening of normal controls. *Arch Gen Psychiatry*. 1991;48:1022-1025.
35. Pujol J, Lopez-Sala A, Deus J, Cardoner N, Sebastian-Galles N, Conesa G, Capdevila A. The lateral asymmetry of the human brain studied by volumetric magnetic resonance imaging. *Neuroimage*. 2002;17:670-679.
36. Pujol J, Cardoner N, Benlloch L, Urretavizcaya M, Deus J, Losilla JM, Capdevila A, Vallejo J. CSF spaces of the Sylvian fissure region in severe melancholic depression. *Neuroimage*. 2002;15:103-106.
37. Good CD, Johnsrude IS, Ashburner J, Henson RN, Friston KJ, Frackowiak RS. A voxel-based morphometric study of ageing in 465 normal adult human brains. *Neuroimage*. 2001;14:21-36.
38. Ashburner J, Neelin P, Collins DL, Evans A, Friston K. Incorporating prior knowledge into image registration. *Neuroimage*. 1997;6:344-352.
39. Ashburner J, Friston KJ. Nonlinear spatial normalization using basis functions. *Hum Brain Mapp*. 1999;7:254-266.
40. Ashburner J, Friston KJ. Voxel-based morphometry: the methods. *Neuroimage*. 2000;11:805-821.
41. Worsley KJ, Marrett S, Neelin P, Vandal AC, Friston KJ, Evans AC. A unified statistical approach for determining significant signals in images of cerebral activation. *Hum Brain Mapp*. 1996;4:58-73.
42. Ashburner J, Friston KJ. Why voxel-based morphometry should be used. *Neuroimage*. 2001;14:1238-1243.
43. Talairach J, Tournoux P. *Co-planar Stereotaxic Atlas of the Human Brain*. New York, NY: Thieme Medical Publishers; 1988.
44. Brett M. The MNI brain and the Talairach atlas [MRC Cognition and Brain Sciences Unit Web site]. Available at: <http://www.mrc-cbu.cam.ac.uk/Imaging/Common/mnispac.html>. Accessed January 16, 2004.
45. Hulshoff Pol HE, Schnack HG, Mandl RC, van Haren NE, Koning H, Collins DL, Evans AC, Kahn RS. Focal gray matter density changes in schizophrenia. *Arch Gen Psychiatry*. 2001;58:1118-1125.
46. Rapoport JL, Wise SP. Obsessive-compulsive disorder: evidence for basal ganglia dysfunction. *Psychopharmacol Bull*. 1988;24:380-384.
47. Modell JG, Mountz JM, Curtis GC, Greden JF. Neurophysiologic dysfunction in basal ganglia/limbic striatal and thalamocortical circuits as a pathogenetic mechanism of obsessive-compulsive disorder. *J Neuropsychiatry Clin Neurosci*. 1989;1:27-36.
48. Baxter LR Jr, Schwartz JM, Bergman KS, Szuba MP, Guze BH, Mazziotta JC, Alazraki A, Selin CE, Ferng HK, Munford P, Phelps ME. Caudate glucose metabolic rate changes with both drug and behavior therapy for obsessive-compulsive disorder. *Arch Gen Psychiatry*. 1992;49:681-689.
49. Rauch SL, Whalen PJ, Dougherty D, Jenike MA. Neurobiologic models of obsessive-compulsive disorder. In: Jenike MA, Baer L, Minichiello WE, eds. *Obsessive-compulsive Disorder: Practical Management*. St Louis, Mo: Mosby-Year Book Inc; 1998:222-253.
50. Middleton FA, Strick PL. Basal ganglia and cerebellar loops: motor and cognitive circuits. *Brain Res Brain Res Rev*. 2000;31:236-250.
51. Leiner HC, Leiner AL, Dow RS. Cognitive and language functions of the human cerebellum. *Trends Neurosci*. 1993;16:444-447.
52. Schmahmann JD. The role of the cerebellum in affect and psychosis. *J Neuro-linguist*. 2000;13:189-214.
53. Schnitzler A, Seitz RJ, Freund HJ. The somatosensory system. In: Toga AW, Mazziotta JC, eds. *Brain Mapping: The Systems*. San Diego, Calif: Academic Press; 2000:291-329.
54. Yeterian EH, Pandya DN. Striatal connections of the parietal association cortices in rhesus monkeys. *J Comp Neurol*. 1993;332:175-197.
55. Wright CI, Groenewegen HJ. Patterns of overlap and segregation between insular cortical, intermediodorsal thalamic and basal amygdaloid afferents in the nucleus accumbens of the rat. *Neuroscience*. 1996;73:359-373.
56. Pujol J, Bello J, Deus J, Cardoner N, Marti-Vilalta JL, Capdevila A. Beck Depression Inventory factors related to demyelinating lesions of the left arcuate fasciculus region. *Psychiatry Res*. 2000;99:151-159.
57. Gur RE, Maany V, Mozley PD, Swanson C, Bilker W, Gur RC. Subcortical MRI volumes in neuroleptic-naive and treated patients with schizophrenia. *Am J Psychiatry*. 1998;155:1711-1717.